Received: 28 January 2022 | Revised: 9 March 2022 | Accepted: 11 March 2022

DOI: 10.1002/app.52839

RESEARCH ARTICLE

Applied Polymer Science WILEY

Cellulose nanocrystals and snail shell-reinforced polyvinyl alcohol bioplastic films: Additive concentration optimization and mechanical properties assessment

Oluwatoyin J. Gbadeyan[1,2,3] | **Olajumoke D. Fagbemi**[2,3] | **Jerome Andrew**[3] | **Sarp Adali**[1] | **Bright Glen**[1] | **Bruce Sithole**[2,3]

[1]School of Engineering, Discipline of Mechanical Engineering, University of Kwazulu-Natal, Durban, South Africa

[2]School of Engineering, Discipline of Chemical Engineering, University of Kwazulu-Natal, Durban, South Africa

[3]Biorefinery Industry Development Facility, Council for Scientific and Industrial Research, Durban, South Africa

Correspondence
Oluwatoyin J. Gbadeyan, School of Engineering, Discipline of Chemical Engineering, University of Kwazulu-Natal, South Africa.
Email: gbadeyano@ukzn.ac.za

Abstract

This study focused on modeling and optimization of the concentration of poly (vinyl alcohol) (PVA), cellulose nanocrystals (CNC), snail shell nanoparticles (SSN), and glycerol for the development of bioplastic films. The response surface methodology using Box–Behnken experimental design was used to investigate the effect of the independent parameters (additives concentrations) on the ultimate tensile strength and Young's modulus of fabricated bioplastic films. A varied ultimate tensile strength and Young's modulus with different component loadings was observed, proving the effect of nanoparticles loading effect on the mechanical properties of bioplastic films. The quadratic polynomial model experiment data provided a coefficient of determination (R^2) of 0.795 for ultimate tensile strength and 0.732 for Young's modulus, evidencing the fitness of the models to pilot the optimization space. The optimum parameters were PVA (7.820%), CNC (1079%), SSN (1241%), and glycerol (2.657%). The ultimate tensile strength and Young's modulus of 27.2 MPa and 31.2 MPa were obtained for the developed bioplastic film with optimized concentrations of each component. The bioplastic films showed improved thermal stability and degradation. The scanning electron microscopy (SEM) imaging revealed a homogeneous dispersion of SSN and CNC in the matrix, which explained the improved properties observed.

KEYWORDS

biomaterials, cellulose and other wood products, morphology, mechanical properties, thermal properties

1 | INTRODUCTION

The increase in demand for package materials has exponentially raised the production of plastic in recent decades. This plastic is synthetic, semi-synthetic, or bio-based, synthesized from either petrochemical (hydrocarbon) or biomass feedstocks.[1–3] The physical properties of plastics, such as being lightweight, make them a perfect fit for food and medicine packaging applications. Consequently, this has led to increased demand for plastic-based packaging

material globally. According to the Grand View research report in 2020,[4] the global market size for plastic packaging was valued at US$ 348.08 billion in 2020 and is predicted to increase at a compound annual growth rate (CAGR) of 4.2% from 2021 to 2028. This expected annual increase is attributed to the swiftly growing demand for plastic packaging in vital applications such as personal and household care, food and beverages, and pharmaceutical industries. However, most readily available plastic materials are developed from synthetic materials. Due to their lightweight, they are easily transported by wind over long distances and dispersed into the environment. This transborder movement of these plastics results in a high degree of pollution on land and water.[5,6] The increased awareness of environmental pollution has led to the need to source plastic from biodegradable and natural resources such as agricultural waste to mitigate the negative effect of plastic end-life on the environment. In the recent years, biomass has been used as a vital raw material feedstock for developing bio-based and biodegradable plastic materials.

Although synthetic polymers such as poly(vinyl alcohol) (PVA) and poly(glycolic acid) (PGA) originate from petrochemical resources, they are non-toxic, biocompatible, biodegradable, and, as a result, are considered biobased plastics.[7–9] They have been used the raw materials to develop different biofilms and show promising potential.[7–9] However, these biobased plastics exhibit poor mechanical performance compared to other synthetic polymers,[7] and many studies have focused on ways to reinforce their mechanical properties.[10–13] Improvements in the mechanical and physical properties of bioplastic films have been reported after incorporating fillers.[14–17] However, these properties remain inferior compared to synthetic-based films. Despite huge bioplastic films developed, there is no study where snail shell nanoparticles (SSN), CNC, and PVA are combined to fabricate bioplastic film.

In this study, this research is fully explored. Snail shell nanoparticles and CNC were hybridized and incorporated as fillers into PVA to develop bioplastic films with improved tensile strength and modulus of elasticity. Poly (vinyl alcohol) was selected as the binder because it is one of the most abundant biopolymers globally, readily available at a cheaper cost. Snail shell nanoparticles and CNC are used as fillers due to their inherent properties availability, adding value to materials regarded as waste and naturally sourced. CNC has superior mechanical, rheological, and optical properties. Its strength has been comparable to Kevlar and widely investigated in the reinforcement of bionanocomposites.[18–21] These confirm the reinforcement ability to add CNC to improve the properties of polymeric materials. Besides, the reinforcement potential of the *Achatina Fulica snail* shell particles has been determined in the recent studies.[22–24] Thus, combining these prominent reinforcements into PVA is expected to produce a final product (bioplastic films) with improved properties. However, investigating the optimized loading portion of these additives to manufacture bioplastic film with excellent properties is needed. In this regard, the primary aim of this study was to optimize the loading concentration of the individual fillers and a combination of both fillers on the mechanical pulling strength and stiffness of SSN and CNC-reinforced bioplastic films. The concentration of PVA, SSN, and CNC was varied according to the Box–Behnken experimental design. The effect of the parameters tested was envisaged by a response surface methodology (RSM) design of experiments. Concentration parameters for PVA were varied between 5 and 10 wt%, SSN 0–5 wt%, CNC 0–5 wt% and glycerol 2–5 wt%. Optimized bioplastic films were characterized using FTIR, SEM, and TGA.

2 | EXPERIMENTAL

2.1 | Materials

Poly (vinyl alcohol) purchased from Sigma-Aldrich, USA was used as a binder. It had an average of 130,000 Mw and was 99% hydrolyzed. Cellulose nanocrystals were supplied by the CSIR, South Africa, and were produced from sawdust using an in-house method as reinforcement. Snail shell nanoparticles were made from *Achatina Fulica* shells using mechano-chemical techniques reported previously.[23] The particle size of nano-$CaCO_3$ from the *Achatina Fulica* shell used for the study ranged from 25 to 64 nm. Nano-$CaCO_3$ was used as reinforcement to hybridize CNC and to enhance the interfacial bonding of bioplastic components. Glycerol was obtained from Sigma-Aldrich (USA) and was used as a plasticizer.

2.2 | Methods

2.2.1 | Experimental design and optimization of bioplastic film production

Design expert software was used to design the experiments using the Box–Behnken experimental design. Four independent variables ranging between 5 and 10 wt.% for PVA, 0–5 wt.% for CNC, 0–5 wt.% for SSN, and 2–5 wt.% for glycerol was used, with the tensile strength and Young's modulus of elasticity chosen as the dependent/response variables. Based on this, the design expert software-generated 29 experimental runs, as shown in Table 1.

TABLE 1 Box–Benken experimental design for bioplastic films

Runs	A: (PVA) wt%	B: (CNC) wt%	C: (SSN) wt%	D: (glycerol) wt%	Response 1: Young's modulus (MPa)	Response 2: tensile strength (MPa)
1	5	2.5	0	3.5	6.5	13.9
2	5	2.5	2.5	5	34.8	12.3
3	7.5	0	2.5	5	32.2	16.2
4	7.5	2.5	2.5	3.5	25.7	33
5	5	2.5	2.5	2	20.6	14.2
6	5	5	2.5	3.5	26.5	16.4
7	10	0	2.5	3.5	27.5	19.2
8	7.5	2.5	2.5	3.5	27	31.1
9	10	2.5	2.5	2	31.4	24.1
10	10	5	2.5	3.5	8.3	9.7
11	10	2.5	0	3.5	23.5	9.1
12	7.5	5	2.5	2	25.8	13.7
13	7.5	0	2.5	2	32.6	12.6
14	7.5	0	0	3.5	24.8	18.4
15	10	2.5	5	3.5	9.4	9.1
16	7.5	0	5	3.5	29.4	17.6
17	7.5	2.5	2.5	3.5	28.5	32.1
18	7.5	5	5	3.5	17.7	14.2
19	7.5	2.5	0	5	26.4	15.4
20	7.5	5	0	3.5	25.2	9.6
21	5	0	2.5	3.5	30.5	21.3
22	7.5	2.5	2.5	3.5	35.4	32.5
23	10	2.5	2.5	5	28.6	18.6
24	7.5	5	2.5	5	32.8	16.5
25	5	2.5	5	3.5	34.7	22
26	7.5	2.5	5	5	29.3	17.7
27	7.5	2.5	0	2	21.7	22.8
28	7.5	2.5	5	2	30.7	25.4
29	7.5	2.5	2.5	3.5	33.2	32.4

The experimental data were fitted to the polynomial quadratic model equation to relate the independent and the response variables, according to Equation (1).

$$Y = \partial_0 + \partial_1 X_1 + \partial_2 X_2 + \partial_3 X_3 + \partial_4 X_4 + \partial_{12} X_1 X_2 + \partial_{13} X_1 X_3 + \partial_{13} X_1 X_4 + \partial_{15} X_2 X_3 + \partial_{23} X_2 X_4 + \partial_{24} X_3 X_4 + \partial_{11} {X_1}^2 + \partial_{22} {X_2}^2 + \partial_{33} {X_3}^2 + \partial_{44} {X_4}^2 \quad (1)$$

where Y represented the response outputs and ∂_0 the intercept, the linear coefficient was obtained from $\partial_1 X_1$ to $\partial_4 X_4$, while $\partial_{12} X_1 X_2$ to $\partial_{23} X_2 X_4$ represented the interactive coefficients and $\partial_{11} {X_1}^2$ to $\partial_{44} {X_4}^2$ the quadratic coefficients. The significance authentication of the model was evaluated by analyzing variance (ANOVA). Three-dimensional response surface plots were produced to study the interaction of one parameter with another.

2.2.2 | Development of bioplastic films

Cellulose nanocrystals and snail shell-filled poly(vinyl alcohol) bioplastic films were fabricated using the solvent casting technique. The process was undertaken in three phases. The first phase was the dissolution of PVA in distilled water. The second was homogenous dispersion of the nanoparticles in the dissolved bio-based polymer solution. The third phase was casting and de-molding of bioplastic films. In the first phase, 250 ml of 5–10 wt% PVA and distilled water solutions were prepared. The pre-calculated

concentration of PVA was measured into a round-bottom flask using a Snowrex digital electronic scale.

Deionized water was measured to complete 100% of the PVA/water solution using a volumetric cylinder and was poured into the round bottom flask. At the same time, an oil bath was heated to 80°C. When the temperature stabilized, the round bottom flask containing the PVA/distilled water solution was immersed into the oil bath and held in position using a retort stand. An overhead mechanical stirrer set at 1000 rpm was used to stir the contents of the round bottom flask for a reaction time of 2 h. In the second phase, the PVA solution was combined with CNC and SSN in a beaker according to the experimental design shown in Table 1. The beaker was then heated on a hot plate to 65°C with stirring at 500 rpm for 1 h to facilitate homogeneous dispersion of the PVA, CNC, and SSN. On completion of the reaction time, the blend was poured into a plastic mold coated with wax and cured for 72 hours at ambient temperature. However, characterization of the bioplastic films was carried out after 2 weeks to ensure adequate curing.

2.2.3 | Measurement of tensile strength and Young's modulus

The tensile strength and Young's modulus of the bioplastic films were determined using a universal testing machine (Instron 5966-K8883, Norwood, USA) fitted with a 10 kN load cell. Five samples of 10 mm width and 25 mm length were tested at an ambient temperature, using a 50 mm/min constant cross-head speed. The average value of the five measurements was reported.

2.2.4 | Fourier-transform infrared spectroscopic analysis

Functional group analysis of the bioplastic films was determined using Fourier-transform infrared spectroscopy (FTIR) spectroscopy (PerkinElmer, USA). A universal attenuated total reflectance module was used for the spectra of the analyzed samples in a wavenumber range between 4000 and 600 cm^{-1}.

2.3 | Thermal properties

Thermogravimetric (TGA) analysis of the bioplastic films was conducted simultaneously using a thermal analyzer (NETZSCH STA-409, USA). The investigation was conducted under an inert atmosphere using dry nitrogen gas set at a 100 ml/min flow rate. Heating was carried out from 30°C to 400°C, using a 10°C/min heating rate. Thermogravimetric analysis was conducted to determine the thermal stability and material degradation of the developed bioplastic films.

2.3.1 | Transmission electron microscope (TEM) investigation

The morphology of CNC and SSN in terms of size and shape was observed under a transmission electron microscope (TEM). The investigation was conducted on TEM Joel 2100 (Japan). About 10 ml of dilute suspensions of CNC was placed on formvar-coated grids, stained with a 2% uranyl acetate solution for 10 min. SSN was prepared for morphology investigation by dispersing 10 ml of snail shells nanoparticle in ethanol and sonicated at 10 kV for 10 min. Afterward, a thin cross-section of cryo-microtomed specimens was prepared using a Leica microtome and placed on carbon copper grids. TEM image of these samples was captured at 100 kV at different magnifications (5000–25,000). The TEM image was further analyzed on the iTEM analyzer software, version 5.0.1 (Japan), to determine the range of particle sizes.

2.3.2 | Scanning electron microscopy (SEM) analysis

The bioplastic film microstructural properties were investigated to determine the mechanism that governs the development of the film's properties. This investigation was achieved by first coating the surface of the films using a Quorum K550x gold sputter coater (PerkinElmer, USA) at 25 mA. The gold-coated films were then observed using a Phenom Pharos Desktop SEM (PerkinElmer, USA) using an accelerating voltage of 10 kV at ambient temperature.

3 | RESULTS AND DISCUSSION

3.1 | Optimization of bioplastic and nanofillers for fabrications of bioplastic films

The tensile strengths and Young's moduli of the fabricated bioplastic films are shown in Table 1 for the different concentrations of PVA, glycerol, CNC, and SSN. These results were then used to formulate the second-order polynomial equations (See Equations (2) and (3)), showing the relationship between the tensile strength and Young's modulus of the bioplastic films and the different constituents.

TABLE 2 ANOVA for ultimate tensile strength and Young's modulus of bioplastic films

Source	Sum of squares	dF	Mean squares	*F*-value	*P*-values	R^2
Ultimate tensile strength (model)	1367.89	14	97.70	5.32	0.0017	0.8419
Young's modulus (model)	1235.69	14	88.26	3.74	0.0096	0.7888

Abbreviation: R2, coefficient of determination; *F*-value: Fisher-snedecor distribution value; df, degree of freedom; *P*-value, probability value.

TABLE 3 Showing model's coefficients of estimates with standard errors

Factor	Ultimate tensile strength CE	Ultimate tensile strength SE	Young's modulus CE	Young's modulus SE
Intercept	29.96	1.92	32.22	2.17
A-PVA	−2.08	1.24	−0.8583	1.40
B-CNC	−3.39	1.24	−2.10	1.40
C-SSCC	1.93	1.24	1.40	1.40
D-GLYCEROL	1.78	1.24	−1.34	1.40
AB	−3.80	2.14	−1.15	2.43
AC	−10.57	2.14	−2.02	2.43
AD	−4.25	2.14	−0.9000	2.43
BC	−3.02	2.14	1.35	2.43
BD	1.85	2.14	−0.2000	2.43
CD	−1.53	2.14	−0.0750	2.43
A^2	−5.15	1.68	−8.62	1.91
B^2	−1.27	1.68	−9.18	1.91
C^2	−5.52	1.68	−7.96	1.91
D^2	2.93	1.68	−6.17	1.91

$$\begin{aligned}\text{Tensile strength (MPa)} = {} & +32.22 - 0.858333A - 2.1B \\ & + 1.4C - 1.34167D - 1.15AB \\ & - 2.025AC - 0.9\,AD + 1.35BC \\ & - 0.2BD - 0.075CD - 8.6225A^2 \\ & - 9.185B^2 - 7.96C^2 - 6.1725\,D^2 \end{aligned} \quad (2)$$

$$\begin{aligned}\text{Young}'\text{s modulus (MPa)} = {} & +29.96 - 2.075A - 3.39167B \\ & + 1.925C + 1.775D - 3.8AB + \\ & - 10.575AC + -4.25AD \\ & - 3,025BC + 1.85BD \\ & - 1.525CD - 5.14667A^2 \\ & - 1,27167B^2 - 5.52167\,C^2 \\ & + 2.92833D^2 \end{aligned} \quad (3)$$

where *A*, *B*, *C*, and *D* represent the percentage concentration of PVA, CNC, SSN, and glycerol, respectively.

The validity of the close-fitting model was then determined using ANOVA, and the results are presented in Tables 2 and 3. Table 2 shows that the tensile strength and Young's modulus of the bioplastic films exhibited high F-values of 5.32 and 3,74 with corresponding low *p*-values of 0.0017 and 0.0096. Meanwhile, the coefficient of determination (R^2) values obtained for the two models were 0.8417 (for tensile strength) and 0.7888 (for Young's modulus), indicating that the models could account for up to 84% and 79% of the variations in the experimental output, respectively.

3.2 | The influence and interaction effects of parameters on tensile strength and Young's modulus

3.2.1 | The interaction effect of PVA and CNC on bioplastic mechanical properties

A significant interaction effect between the concentration of PVA and CNC was observed for tensile strength and Youngs Modulus, as shown in Figures 1a and 2a, respectively. Notably, the lower concentration loading of 2.5 wt% CNC and 7.5 wt% PVA offered a superior tensile strength of 33 MPa. A similar trend was observed in Figure 2a for Youngs Modulus, where the loading of

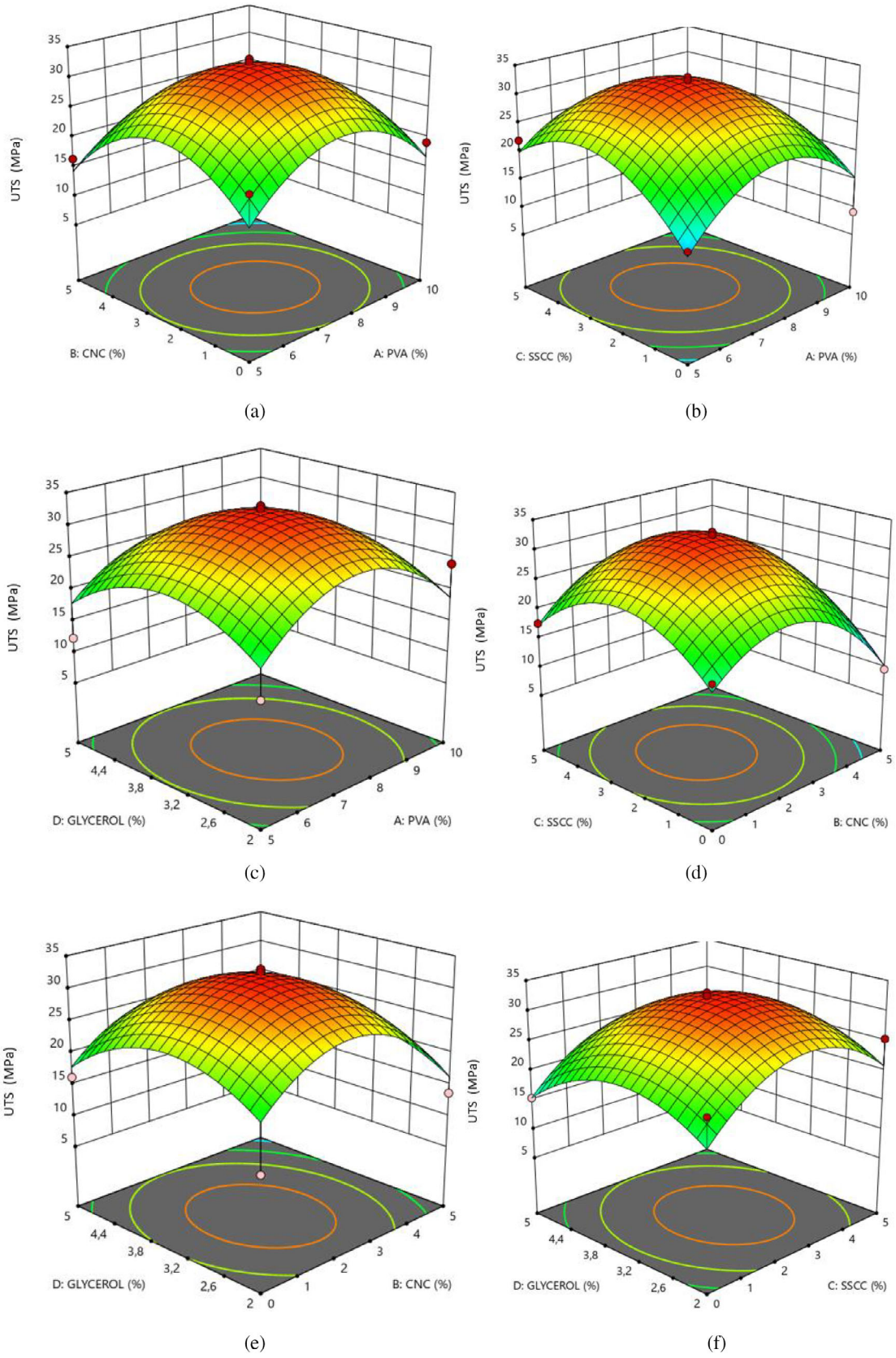

FIGURE 1 The 3-D surface plot of tensile strength as a function of PVA, CNC, SSN and glycerol concentrations: Interaction effects of CNC and PVA (a), SSN and PVA (b), glycerol and PVA (c), SSN and CNC (d), glycerol and CNC (e), and glycerol and SSN (f) [Color figure can be viewed at wileyonlinelibrary.com]

2.5 wt%. CNC and 7.5 wt% PVA resulted in a maximum Young's modulus of 35 MPa, indicating the optimal concentration of PVA and CNC for superior mechanical properties. These results were consistent with the findings of Yang et al., where the loading of CNC was found to improve the PVA tensile strength from 264 MPa to 35.4 MPa.[25] This significant improvement in mechanical properties may be attributed to the reinforcing effect of nanoparticles incorporated at low concentrations.[26,27] A sharp drop in tensile strength at the loading of CNC above 2.5 wt.% may be attributed to aggregation of the nanoparticles and the loading effect of the other components, producing a weaker structure and resulting in reduced tensile strength and Young's modulus.

3.2.2 | The interaction effect of SSN and PVA on bioplastic mechanical properties

Figures 1b and 2b show the interaction effects of SSN and PVA on the mechanical properties of the bioplastic films. It was observed that the interaction of SSN and PVA was similar to the CNC and PVA interaction, shown in Figures 1a and 2a. The combination of 7. About 5 wt% of PVA and 2.5 wt% of SSN exhibited a superior tensile strength of 33 MPa and 35.4 MPa for Young's modulus. This combination was identified as optimum based on the concentration of glycerol and CNC, which was 3.5 wt%. and 2.5 wt%. The use of SSN has been reported in previous studies to have a strong reinforcement influence on mechanical properties.[27,28] Uniform dispersion of the nanoparticles in the matrix of the films (Figure 3) provided for a more robust structure with high resistance to pulling stress, resulting in increased mechanical properties.

3.2.3 | The interaction effect of glycerol and PVA on bioplastic mechanical properties

Glycerol was used as a plasticizer to increase the flexibility of PVA film in combination with the other components used to fabricate the bioplastic films. Figures 1c and 2c show the interaction effect of glycerol and PVA on the mechanical properties of the bioplastic films. The results showed that the concentration of glycerol had a reflective impact on the mechanical properties of the bioplastic film. An improved tensile strength (33 MPa) and Young's modulus (35.4 MPa) were observed at 7.5 wt%. PVA and 3.5 wt% glycerol was combined. A decrease in mechanical strength and increased film stiffness were observed when glycerol was above 3.5 wt%. This result is consistent with other studies, showing that high plasticizer concentrations resulted in decreased mechanical properties.[29,30]

3.2.4 | The interaction effect of SSN and CNC on bioplastic mechanical properties

The interaction of the two primary reinforcing nanoparticles (SSN and CNC) on the mechanical properties of the bioplastic films are shown in Figures 1d and 2d. It was observed that a small loading (2.5 wt%) of both reinforcement nanoparticles improved the mechanical properties of the films. This performance again illustrated the effectiveness of loading small quantities of nanoparticles. This performance may be attributed to both materials being carbon-based materials, with catenation capability. It may be that these two additives increased the chemical linkage into chains of atoms of the same element, forming relatively strong bonds with it and other components, resulting in better resistance of films to external pulling stress.[31] The compatibility of these reinforcements is another reason for improved mechanical strength and stiffness observed. Both fillers are naturally sourced, with the similar elemental components forming a hybrid structure component with high mechanical properties. The improvement of mechanical strength is well established when using SSN and CNC to fabricate composite films.[31–33]

3.2.5 | The interaction effect of glycerol and CNC on bioplastic mechanical properties

The interaction effect of loading glycerol and CNC for the fabrication of bioplastic films is shown in Figures 1e and 2e. Low concentrations of both components offered significant improvement in the mechanical properties of the films. Significantly, the loading of 2.5 wt% CNC and 3.5 wt% glycerol showed a tensile strength and Young's modulus of 33 and 35.4 MPa. This result complemented the results shown in Figures 1 and 2 (a, b, c, and d), where higher tensile strength and Young's modulus of 33 and 35.4 MPa were obtained, which shows the consistency in the result and validates the optimum concentration of CNC and glycerol at 2.5 wt% and 3.5 wt% for bioplastic film development.

3.2.6 | The interaction effect of glycerol and SSN on bioplastic mechanical properties

Figures 1f and 2f show the loading interaction effect of glycerol and SSN on the fabricated bioplastic films. It was observed that loading of 2.5 wt% CNC and 3.5 wt%

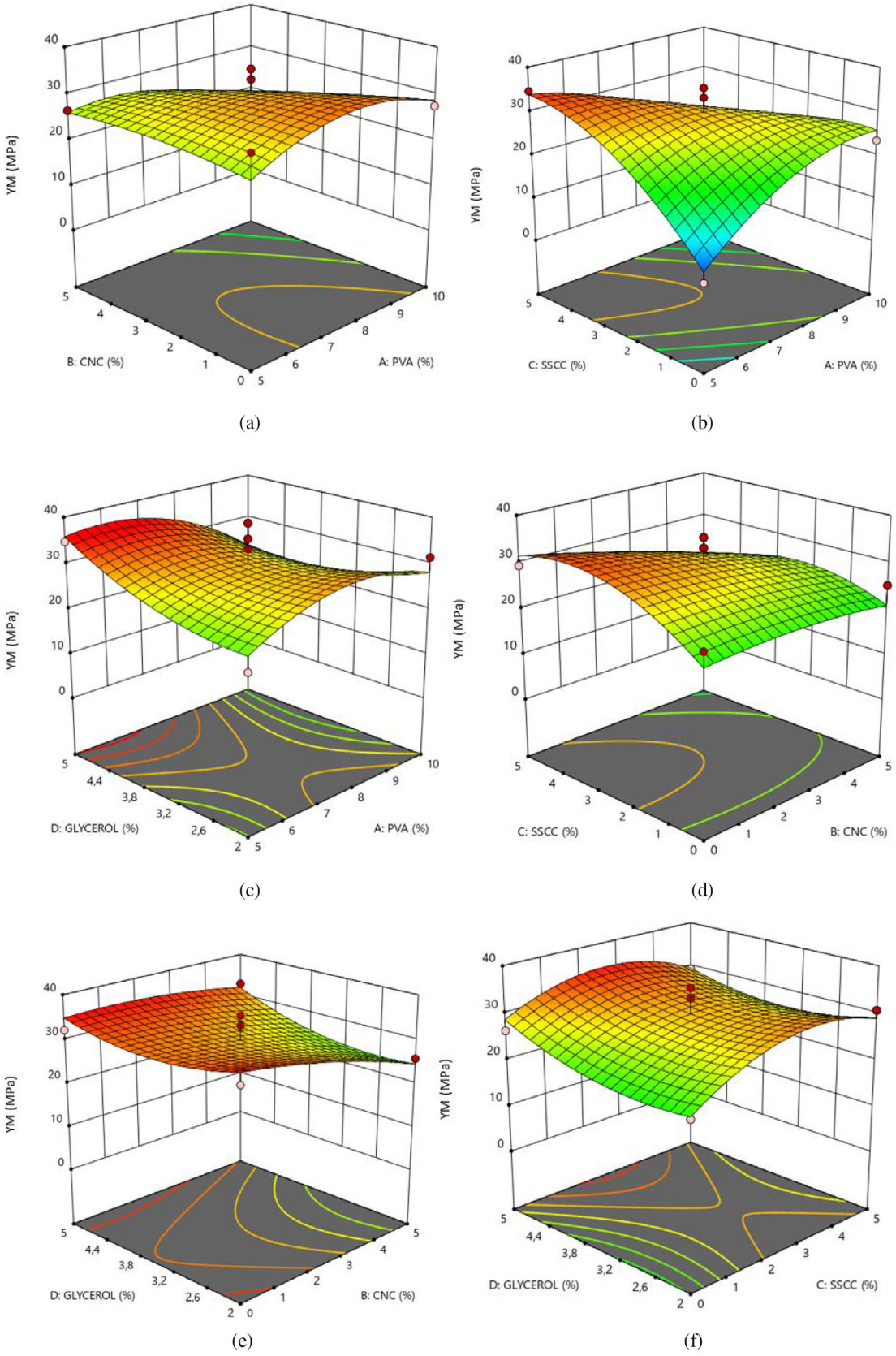

FIGURE 2 The 3D surface plot of Young's modulus as a function of PVA, CNC, SSN and glycerol concentrations: Interaction effects of CNC and PVA (a); SSN and PVA (b); glycerol and PVA (c); SSN and CNC (d); glycerol and CNC (e); and glycerol and SSN (f) [Color figure can be viewed at wileyonlinelibrary.com]

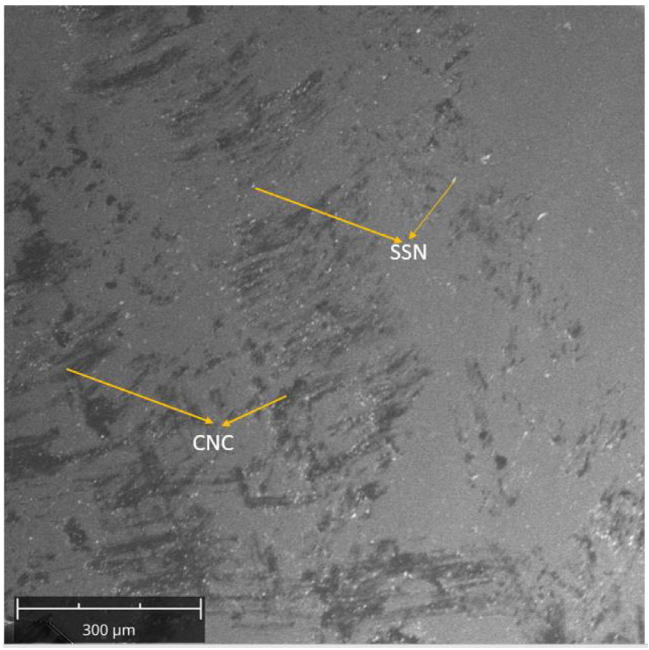

FIGURE 3 Scanning electron microscopy (SEM) micrographs showing the surface microstructure of bioplastic film [Color figure can be viewed at wileyonlinelibrary.com]

glycerol offered superior properties. This trend was similar to that observed in Figures 1e and 2e.

3.3 | Validation of ultimate tensile strength and Young's modulus of the developed bioplastic films

The optimal setpoints related to the model shown in Table 4 include PVA (7.820%), CNC (1079%), SSN (1241%), and glycerol (2.657%). The optimized process conditions for bioplastic films based on the model predicted a tensile strength. Young's modulus of 26,853 and 29.242 MPa shown in Figure 5 are optimal mechanical properties. The validation of values obtained from the software was experimentally conducted in triplicate to confirm its accuracy. Average tensile strength of 27.2 MPa and Young's modulus of 31.19 MPa was obtained, as shown in Table 4 (Table 5).

3.4 | Characterization

3.4.1 | Microstructure of bioplastic film

Scanning electron microscopy (SEM) was used to determine the fracture mechanism of the bioplastic films. Figure 3 shows the SEM image of the surface of the developed films. Homogeneous distribution of filler (SSN and CNC) firmly bonded within the matrix, resulting in a relatively smooth surface. This structural formulation may be attributed to improved tensile strength and Young modulus. The loading of SSN and CNC may provide an interlocking structure that induces higher strain and ability to bear a higher load, resulting in increased strength and Young's modulus (Figure 4).

TABLE 4 Optimum loading variables for ultimate tensile strength and Young's modulus of bioplastic films

Independent variables	Predicted optimum levels (%)
Poly (vinyl alcohol)	7820
Cellulose nanocrystals	*1079*
Snail shell nanoparticle	1241
Glycerol	*2657*

TABLE 5 Predicted and observed values for ultimate tensile strength and Young's modulus of bioplastic films

Responses	*Predicted values (MPa)*	*Observed values (MPa)*
Tensile strength (model)	26.853	*27.2*
Young's modulus (model)	29.242	*31.19*

Microstructure of SSN and CNC

TEM images CNC and SSN analyzed under TEM image analyzer software version 5.0.1 were reported in our previous studies.[23,34] Figure 2 shows the TEM image analysis for 20 counts of CNC and SSN particle sizes. The rod-like morphology of the CNC particles is evident, with dimensions ranging from 100 to 200 nm in length and 10–20 nm in width. Furthermore, the means of the SSN powder shown in Figure 2b consisted of 25.35–63.68 nm sizes of a particle having semi-sphere morphology. The TEM micrograph shown in Figure 2a revealed a rod-like morphology of the CNC particles with dimensions ranging from 100 to 200 nm in length and 10–20 nm in width. The morphology and particle size of CNC and SSN are crucial as they provide a more precise understanding of the reinforcement role of CNC and interfacial adhesion provided by SSN used as reinforcement filler. SSN is purely calcium carbonate that enhances CNC bonding to the binder, producing a more robust structure with high resistance to an external pulling force. It also observed that the CNC image obtained shows mostly individual nanocrystals and some aggregates, which may be due to the high density of the hydroxyl groups on the surface of the cellulose chain molecules, resulting in the formation of hydrogen. This formation forms good interaction with

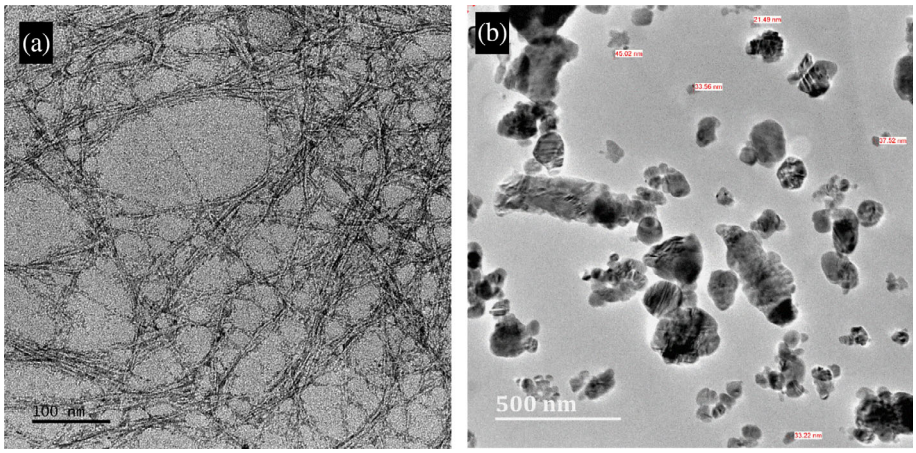

FIGURE 4 SEM micrographs showing structure and morphology of (a) CNC (b) SSN [Color figure can be viewed at wileyonlinelibrary.com]

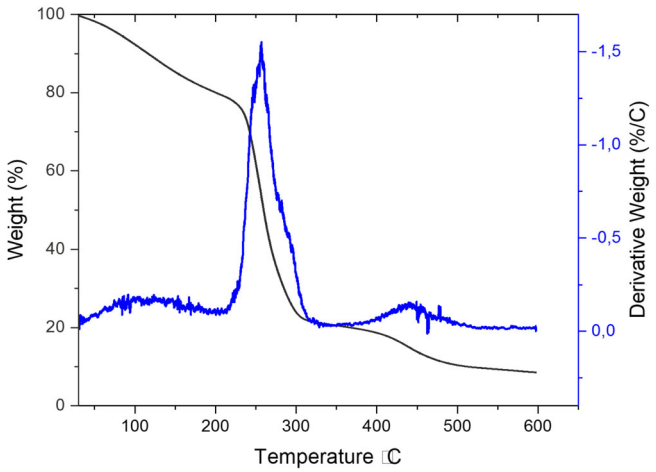

FIGURE 5 TGA thermogram curve of bioplastic film [Color figure can be viewed at wileyonlinelibrary.com]

carbon single-bonded oxygen stretching in-plane carbon and single-bonded hydroxyl bending in carboxylic acids shown in Figure 5, leading to the suitable structural formulation for improved mechanical properties.

3.4.2 | Thermal properties

The thermal stability and degradation of the bioplastic films with an optimal concentration of PVA, SSN, CNC, and glycerol are shown in Figure 5. A minor weight loss (0.06%) was observed between 30°C and 100°C and was attributed to evaporation and loss of moisture. After that, three thermal occurrences were observed within the temperature range of 100–400 °C. The first phase (100–248°C) was exothermic, with a weight loss of up to 21%. This material degradation may be linked to the depolymerization of the PVA.[14]

The second phase (phase (249–310°C) corresponds with the disintegration of organic materials such as CNC and SSN in the bioplastic films.[35] The weight loss in this phase equated to 87%. The third phase (310–400°C) was a further endothermic decomposition of carbon dioxide to calcium oxide (ashes), which amounted to about 10% weight loss. The thermal properties observed for the bioplastic films from PVA reinforced with SSN and CNC exhibited superior properties than PVA reinforced with biochar nanoparticles reported by Nan et al.[14]

3.4.3 | Fourier-transform infrared spectrometry

The FTIR spectrum of the bioplastic films fabricated with optimum concentrations of PVA, SSN, CNC, and glycerol is shown in Figure 6. Several peaks were observed within the range of 550–4000 cm^{-1}. A broad and medium intensity band was observed at 3272 cm^{-1} due to the O—H stretching. O—H stretching relates to the macromolecules of CNC synthesized from wood and is also characteristic of SSN and PVA elemental composition.[36]

The stretching vibration of O—H may be due to the intra- and extra-molecular hydrogen bonding from the covalent bonds between the molecules of the additives.[20] The peak at 2921 cm^{-1} was associated with CH_2 stretching vibration presenting the distinctive feature of CNC. It is also associated with the silanol band in the materials.[21–23] Furthermore, the bands at 2921 cm^{-1} and 2854 cm^{-1} correspond to the asymmetric and symmetric vibration stretching of aliphatic C—H, showing that bioplastic film contains carbon and hydrogen together in straight chains. Moreover, a very prominent absorption peak was observed at 1652 cm^{-1}, associated with the C═C stretching of conjugated alkenes. The peak at 1455 cm^{-1} due to O—H bending of carboxylic acid 1090 cm^{-1} is associated with C-O stretching of a primary alcohol, which may be related to the PVA present in the material. The absorption peaks at 1042, 916.92, and 842 cm^{-1} were associated with the

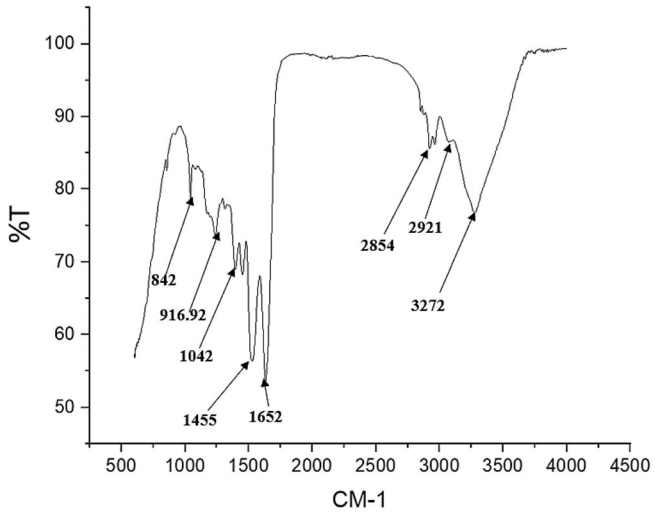

FIGURE 6 Fourier-transforms infrared (FTIR) spectra of bioplastic film

presence of carbonates ions related to the SSN in the film.[24] Most of the spectrum displayed a leading band that indicates the interaction between carbon single-bonded oxygen stretching in-plane carbon and single-bonded hydroxyl bending in carboxylic acids, which are the leading functional group of the bioplastic film developed.

4 | CONCLUSIONS

The development process models of bioplastic films relating to the design combination of different concentrations of PVA, CNC, and SSN, glycerol for producing bioplastic films with good ultimate tensile strength and Young's modulus were studied. Four independent variables ranging from 5–10 wt% for PVA, 0–5 wt% for CNC, 0–5 wt% for SSCC, and 2–5 wt% for glycerol were evaluated. The optimum concentration obtained was PVA (7.820%), CNC (1079%), SSN (1241%), and glycerol (2.657%). The ultimate tensile strength and Young's modulus of 27.2 and 31.2 MPa were obtained for the developed bioplastic film with an optimized concentration of components. The estimated mechanical properties setpoints were positively influenced by PVA, CNC, and SSN concentrations. FTIR spectra displayed a leading band that indicated the interaction between carbon single-bonded oxygen stretching in-plane carbon single-bonded hydroxyl bending in carboxylic acids, which are the leading functional group of the bioplastic film developed. This functional group may be the reason for the high ultimate tensile strength and Young's modulus obtained. SEM images reveal uniform dispersion of CNC and SSN in the matrix, which could be associated with better resistance to pulling stress. The characteristic of the developed films is suggestive of materials that may be successfully used for packaging application.

AUTHOR CONTRIBUTIONS

Olajumoke D. Fagbemi: Methodology (equal); software (equal). **Jerome Andrew:** Writing – review and editing (supporting). **Sarp Adali:** Formal analysis (lead); supervision (lead); writing – review and editing (supporting). **Bright Glen:** Funding acquisition (lead); supervision (supporting). **Bruce Sithole:** Resources (equal); supervision (equal); writing – review and editing (equal).

CONFLICT OF INTEREST

The authors declare that they have no known competing financial interests or personal relationships that could have influenced the work reported in this paper.

DATA AVAILABILITY STATEMENT

The data that support the findings of this study are available from the corresponding author upon reasonable request.

ORCID

Oluwatoyin J. Gbadeyan https://orcid.org/0000-0002-7906-3965

REFERENCES

[1] K. Ryder, M. A. Ali, J. Billakanti, A. Carne, *J. Polym. Environ.* **2020**, *28*, 725.
[2] B. V. K. J. Schmidt, *Macromol. Rapid Commun.* **2020**, *41*, 1900333.
[3] S. A. Mason, V. G. Welch, J. Neratko, *Front. Chem. Orig. Res.* **2018**, *6*, 407.
[4] G. V. RESEARCH. Plastic Packaging Market Size, Share & Trends Analysis Report By Product (Flexible, Rigid), By Technology (Extrusion, Thermoforming), By Application (Food & Beverages, Pharmaceuticals), And Segment Forecasts, 2021–202. https://www.grandviewresearch.com/industry-analysis/plastic-packaging-market#:~:text=The%20global%20plastic%20packaging%20market%20size%20was%20estimated%20at%20US,DUSD%20361.73%20billion%20in%202021.&text=The%20plastic%20packaging%20market%20is,USD%20486.2%20billion%20by%202028.
[5] F. O. Afolabi, P. Musonge, B. F. Bakare, *J. Environ. Health Sci. Eng.* **2021**, *19*, 613.
[6] N. Ramakrishnan, S. Sharma, A. Gupta, B. Y. Alashwal, *Int. J. Biol. Macromol.* **2018**, *111*, 352.
[7] O. V. López, L. A. Castillo, M. A. Garcia, M. A. Villar, S. E. Barbosa, *Food Hydrocolloids* **2015**, *43*, 18.
[8] B. Marelli, N. Patel, T. Duggan, G. Perotto, E. Shirman, C. Li, D. L. Kaplan, F. G. Omenetto, *Proc. Nat. Acad. Sci.* **2017**, *114*, 451.
[9] G. Perotto, R. Simonutti, L. Ceseracciu, M. Mauri, D. Besghini, A. Athanassiou, *Polymer* **2020**, *200*, 122598.
[10] T. Y. Chong, M. C. Law, Y. San Chan, *J. Polym. Environ.* **2021**, *29*, 363.

[11] M. R. Nanda, M. Misra, A. K. Mohanty, *Macromol. Mater. Eng.* **2012**, *297*, 184.
[12] N. E. Wahyuningtiyas, H. Suryanto, *J. Mech. Eng. Sci. Technol.* **2018**, *2*, 20.
[13] M. B. Agustin, B. Ahmmad, S. M. M. Alonzo, F. M. Patriana, *J. Reinf. Plast. Compos.* **2014**, *33*, 2205.
[14] N. Nan, D. B. DeVallance, X. Xie, J. Wang, *J. Compos. Mater.* **2016**, *50*, 1161.
[15] H. Judawisastra, R. Sitohang, L. Marta, Water absorption and its effect on the tensile properties of tapioca starch/polyvinyl alcohol bioplastics. in *IOP Conference Series: Materials Science and Engineering, 2017*, Vol. 223, IOP Publishing, Bristol, England 12066.
[16] S. M. Sa'adah, E. Saepudin, Effect of citric acid on physical and mechanical properties of Starch/PLA/PVA bioplastic films. in *AIP Conference Proceedings*, Vol. 2370, AIP Publishing LLC, Melville, United States **2021**, p. 60011.
[17] R. Lim, P. L. Kiew, M. K. Lam, W. M. Yeoh, M. Y. Ho, *Asia-Pac. J. Chem. Eng.* **2021**, 16, e2622.
[18] W. Bessa, D. Trache, M. Derradji, A. F. Tarchoun, *Defence Technology* **2021**.
[19] W. J. Orts et al., Effect of fiber source on cellulose reinforced polymer nanocomposites. in *ANTEC-CONFERENCE PROCEEDINGS*, Vol. 2, Alabama, USA **2004**, p. 2427.
[20] F. Xie, J. Bao, L. Zhuo, Y. Zhao, W. Dang, L. Si, C. Yao, M. Zhang, Z. Lu, *Carbohydr. Polym.* **2020**, *245*, 116610.
[21] Z. Lu, D. Ning, W. Dang, D. Wang, F. Jia, J. Li, S. E, *Cellulose* **2020**, *27*, 8027.
[22] O. J. Gbadeyan, S. Adali, G. Bright, B. Sithole, A. Omojoola, *Compos. Struct.* **2020**, *239*, 112043.
[23] O. J. Gbadeyan, S. Adali, G. Bright, B. Sithole, S. Onwubu, *J. Nanomater.* **2020**, *2020*. https://doi.org/10.1155/2020/4370172
[24] O. Gbadeyan, S. Adali, G. Bright, B. Sithole, P. Lekha, *J. Compos. Mater*. **2021**, *55*, 3345.
[25] W. Yang, G. Qi, J. M. Kenny, D. Puglia, and P. Ma, *Polymers*, **2020**, *12*, 1364.
[26] J. Xue, T. Wang, Q. Hu, M. Zhou, Y. Luo, *Food Hydrocoll.* **2018**, *79*, 110.
[27] O. J. Gbadeyan, S. Adali, G. Bright, B. Sithole, *NANO* **2021**, *7*, 79.
[28] T. Mohan, K. Kanny, *J. Compos. Mater.* **2018**, *52*, 3989.
[29] P. A. Sreekumar, M. A. Al-Harthi, S. K. De, *J. Appl. Polym. Sci.* **2012**, *123*, 135.
[30] L. Monjazeb Marvdashti, M. Yavarmanesh, A. Koocheki, *Iran. J. Food Sci. Technol. Res.* **2016**, *12*, 663.
[31] O. Gbadeyan, S. Adali, G. Bright, B. Sithole, P. Lekha, *J. Compos. Mater.* **2021**, *55*, 3345.
[32] M.-C. Popescu, *Int. J. Biol. Macromol.* **2017**, *101*, 783.
[33] Z. Jahan, M. B. K. Niazi, Ø. W. Gregersen, *J. Ind. Eng. Chem.* **2018**, *57*, 113.
[34] O. D. Fagbemi, J. E. Andrew, B. Sithole, *Biomass Convers Biorefin.* **2021**, *259*. https://doi.org/10.1007/s13399-021-02015-6
[35] T. Nguyen, E. Zavarin, E. M. Barrall, *J. Macromolec. Sci.—Rev. Macromolec. Chem.* **1981**, *20*, 1.
[36] J. Shi, D. Xing, J. Lia, *Energy Proc.* **2012**, *16*, 758.

How to cite this article: O. J. Gbadeyan, O. D. Fagbemi, J. Andrew, S. Adali, B. Glen, B. Sithole, *J. Appl. Polym. Sci.* **2022**, *139*(36), e52839. https://doi.org/10.1002/app.52839